Effects of nanosecond-pulsed laser irradiation on nanostructure formation on the surface of thin Au films on SiO_2 glass substrates

Ruixuan Yu[1)], Tamaki Shibayama[2)], Xuan Meng[1)], Shinya Takayanagi[1)], Yutaka Yoshida[2)], Shigeo Yatsu[2)], Seiichi Watanabe[2)]

[1)] Graduate School of Engineering, Hokkaido University, Sapporo, Hokkaido 060-8628, Japan

[2)]Center for Advanced Research of Energy and Materials Science,

Faculty of Engineering, Hokkaido University,

Sapporo, Hokkaido 060-8628, Japan

Abstract

In this study, we investigated nanostructure formations on the surface of Au thin films deposited on SiO_2 glass substrates after nanosecond-pulsed laser irradiation, also the correlation between the nanostructures parameters and the photoabsorption peak. Spherical Au nanoparticle/SiO_2 glass nanocomposites were formed on the surface of the Au thin films deposited on the SiO_2 glass substrates after nanosecond-pulsed laser irradiation in air with a wavelength of 532 nm at a repetition rate of 2 Hz and a laser energy density of 0.7 kJ/m^2. Au nanoparticles were periodically arranged on the substrates under laser irradiation perpendicular to the direction of the electrical field vector of the laser light, the average diameter of Au nanoparticles was increased from 59.3 to 67.4 nm and the average distance of the laser induced periodical structure was decreased from 1.3 to 1.0 μm as the number of laser pulses increased from 1000 to 1500. After 2000 pulses irradiation, an additional laser irradiation induced periodical structure was formed in the direction parallel to the electrical field vector of the laser. The average periodicity of this nanostructure perpendicular to the initial nanostructure was 560 nm, which is close to the wavelength of the nanosecond-pulsed laser used in this study. The average diameter of these Au nanoparticles is 41.9 nm which is smaller than that of the Au nanoparticles formed after 1000 pulses irradiation. Au nanoparticles were

generally dispersed on the surface while some were embedded in the substrate. After 1500 pulses irradiation, the diameter of the Au nanoparticles on the Au(30 nm)/SiO_2(0.8 mm) is relatively larger than that of the Au nanoparticles on the Au(20 nm)/SiO_2(0.1 mm). Each of laser irradiated sample showed an own photoabsorption peak clearly in this study. Furthermore, effects of the average diameter of the Au nanoparticles on the photoabsorption peak are discussed.

Keywords:

Laser irradiation, periodic nanostructures, Au nanoparticle, SiO_2 substrates, localized surface plasmon resonance.

Abbreviations:

SEM: scanning electron microscope;

TEM: transmission electron microscopy;

FIB: focused ion beam equipment;

EDS: energy-dispersive spectrometer;

LSPR: localized surface plasmon resonance;

F.C.C: face centered cubic;

ACF: autocorrelation functional;

FFT: fast Fourier transform.

1. **Introduction**

Noble metallic nanoparticle/dielectric systems exhibit nonlinear optical properties such as the well-known localized surface plasmon resonance (LSPR) effect [1]. Therefore, such nanocomposites have applications as biosensors [2-8], waveguides [9], and photocatalysts [10].

Noble metallic nanostructures can be prepared by quantum beam irradiation such as ion implantation or by laser irradiation. One such preparation method employs ion implantation and subsequent thermal annealing, which can control the depth of the embedded nanoparticles in the substrate and the nanoparticle size distribution by implantation energy, ion dose, and various heat treatments after ion implantation as well as the substrate temperature during ion implantation [11-19]. The surface temperature of metal thin films may reach the melting point or the boiling point if the short-pulsed laser power densities are sufficiently high [20]. The melting of metal thin films leads to dewetting processes. Finally surface nanostructures on the substrate can be obtained by Rayleigh instability mechanism [21-23]. In addition, nanostructures with a periodic structure can be obtained by short-pulsed laser irradiation. The surface structure obtained by this method strongly depends on the laser wavelength and electric field vector [24-28]. The Au nanoparticles formation and dispersion on the SiO_2/Si substrate

by short-pulsed laser irradiation induced dewetting process have been reported by S. J. Henley et al. [21] and F. Ruffino et al. [23]. Generation of periodic Au nanostructure in Au nanoparticle-containing polymer films on the glass substrate by short-pulsed laser irradiation has been reported by A. Kiesow et al. [25]. Absorption of laser energy in the nanoparticles results in various effects such as Au submicron lines formation by nanosecond-laser ablation of Au nanoparticle films on polyimide substrate [29], and fragmentation of Au nanoparticles on the glass substrate [30].

In this study, we investigated the formation of Au/SiO_2 nanostructures by nanosecond-pulsed laser irradiation and their resulting optical properties. Moreover, we explored laser irradiation induced periodic nanostructures on the surfaces of Au films deposited on SiO_2 glass substrates and changes in the periodic nanostructure surfaces as a result of varying the number of laser pulses. Optical absorbance measurements were used to explore the optical properties of the Au nanoparticle/SiO_2 glass system and the relationship between the optical properties and nanostructure size.

2. **Experimental procedure**

SiO_2 glass substrates of diameter 10 mm, mirror polished on both sides with an O-H density of 80-100 ppm (Shin-Etsu Chemical Co., Ltd) were used in this study. The thicknesses of the substrates were 0.1 mm (sample 1) and 0.8 mm (sample 2). A thin Au

film was deposited on the SiO_2 glass substrates using a vacuum evaporator at room temperature by electrically heating the Au source (purity, 99.9%) operated at 6.0×10^{-5} Torr. The average thickness of the applied Au layer was 20 nm for sample 1 and 30 nm for sample 2. The thickness of the Au thin films deposited on the glass substrate was estimated by comparing the colors with that of the standard sample which had been previously calibrated. The laser energy absorption of the 30 nm Au thin films would be almost as same as that of the 20 nm Au thin films [21]. So we investigated irradiation effects of the thickness of the Au thin films on nanostructure formation by using the sample 1 and the sample 2.

After nanosecond-pulsed laser irradiation, photoabsorbance measurements and surface morphology examination of the irradiated region were performed for sample 1. Sample 2 was used for cross-sectional microstructural analysis using a transmission electron microscope (TEM: JEOL JEM-2010F). It is hard to prepare the cross-sectional TEM specimen by focused ion beam equipment (FIB: JEOL JEM-9320FIB) from the thin SiO_2 substrate (sample 1), so we made the cross-sectional TEM specimen by FIB from the thick SiO_2 substrate (sample 2). To compare the effects of substrate thickness on absorption of laser beam energy in this study, we tried to observe the irradiated spot. However, we did not observe significant difference of the irradiated spot morphology

between the sample 1 and the sample 2 under our experimental conditions in this study. We concluded that the effects of substrate thickness on the irradiated spot were negligible. Nanosecond-pulsed laser irradiation perpendicular to the sample surface was performed in air at room temperature using a linearly polarized Nd:YAG pulse laser (Inlite Ⅱ, Continuum Co., Ltd) with a wavelength of 532 nm and diameter of about 6 mm. The repetition rate was 2 Hz with a pulse duration time of 5–7 ns. The average laser energy density was 0.7 kJ/m^2.

After laser irradiation, photoabsorbance measurements were performed with a spectrophotometer (JASCO Spectrophotometer V-630); using a slit put on the sample to confine the irradiated region. The surface morphology of the specimen was observed using a scanning electron microscope (SEM: JEOL JSM-7001FA), and cross-sectional microstructural analyses were performed using a TEM. The TEM specimens were prepared using focused ion beam equipment (FIB: JEOL JEM-9320). The elemental concentration was obtained using an energy-dispersive spectroscope (EDS: Noran, Thermo Fischer Scientific) along with the TEM. A detailed study of the Au granules and the Au nanoparticles was conducted by measuring from SEM images by using Mac-view ver.4 software (MOUNTECH Co., Ltd). The Heywood diameter (area equivalent circle's diameter) and the average diameter were applied to Au granules as

ununiform shape and the Au nanoparticles as spherical shape, respectively.

3. **Results and discussion**

3.1 Observation of surface morphology after laser irradiation

Figure 1(a) and (b) show SEM images of the surface morphology of the specimen before nanosecond-pulsed laser irradiation. As increasing the thickness of the Au thin film on the SiO_2 glass substrate from 20 nm (sample 1) to 30 nm (sample 2), the Au granular grains in sample 1 grew to large islands grains. It can be observed that the SiO_2 glass substrate surface was uneven covered with Au granular grains of Heywood diameter 20–50 nm and the mean circularity coefficient of 0.58±0.17 in sample 1. Several cracks in the Au thin foil were also observable before nanosecond-pulsed laser irradiation. The nanosecond-pulsed laser was applied from a direction perpendicular to the Au thin film surface in air at room temperature for 1000, 1500, and 2000 pulses. The nanosecond-pulsed laser was applied from a direction perpendicular to the Au thin film surface of sample 2 in air at room temperature for 1500 pulses. It has been reported that in the beginning of the vacuum-deposition of the Au thin films, the hemispherical Au clusters nucleated and coalesced each other, then laterally grew on the substrate, finally the cracks formed between the granular grains since the thickness of Au thin films reached over about 20 nm or more [31-32].

The thickness of the Au thin films deposited on SiO_2 glass substrate was estimated by comparing the colors with that of the standard sample which had been calibrated. To examine this method, we measured the thickness of the Au thin films deposited on the SiO_2 glass substrate by the cross-sectional TEM image from sample 2 as shown in Fig.1(c) and confirmed that the average thickness of the Au thin films is 30 nm, which is consistent with the thickness obtained by comparing the standard sample. Therefore, it is reliable to determine the average thickness of the Au thin films from the color of the Au thin films.

Figure 2 shows optical microscope images of sample 1 after nanosecond-pulsed laser irradiation for (a) 1000, (b) 1500, and (c) 2000 pulses and those of sample 2 after laser irradiation for (d) 1500 pulses. As can be observed from the figures, the original metallic color of the Au films was replaced by pale transparent red in the irradiated regions. The nominal laser beam spot is 6 mm in diameter. We tried to evaluate the profile of energy distribution in the laser beam used in this study by color change after laser irradiation shown in Figure 2. It was smaller than the diameter of the nominal laser beam spot. Moreover we carefully observed the surface nanostructure on the substrate after laser irradiation. We found the laser induced nanostructure which formed uniformly at the edge of color changed region as shown in yellow open circular region

in Figure 2. The laser induced nanostructure always formed at the same region and reproducibility was excellent in this study. The diameter of that region is about 1 mm. Therefore we used the aperture with 1 mm in diameter to evaluate the photoabsorption peak through the laser induced nanostructure region.

Figure 3 shows photoabsorbance spectra of the laser irradiated region obtained from the yellow open circular region as shown in Figure 2(a)–(d). Figure 3(a)-(c) show the photoabsorbance spectra of the sample 1 after 1000, 1500 and 2000 pulses irradiation, respectively. Figure 3(d) shows the photoabsorbance spectra of the sample 2 after 1500 pulses irradiation. Examination of the data in Figure 3 indicates that absorption peaks at approximately 534, 536, 526 and 540 nm were obtained from the photoabsorbance spectra of Figure 3(a)-(d), respectively. The presence of a photoabsorbance peak due to the LSPR effect indicates that Au/SiO_2 nanocomposite structures were formed by laser irradiation. The LSPR peak wavelength change is due to change in the sizes of the Au nanoparticles [33].

Figures 4 (a)–(c) show SEM images of the sample 1 surface observed after laser irradiation for (a) 1000, (b) 1500, and (c) 2000 pulses. The SEM images were obtained from the laser induced nanostructure at the edge of color changed region as shown in the yellow open circle in Figure 2(a)-(c). Figures 4(a) and (b) show dispersed Au grains

of diameter 20–50 nm after laser irradiation and the formation of periodic nanostructures on the SiO_2 glass substrate surface. The periodic nanostructures can be observed to lie perpendicular to the electric field vector of the linearly polarized laser beam (***E*** vector). As shown in Fig. 4(c), additional periodic nanostructures parallel to the ***E*** vector direction were formed as the irradiation pulses were increased to 2000.

Figures 4(d)–(f) show the autocorrelation functional (ACF) images obtained by the fast Fourier transform (FFT) of the squared part in Figs. 4(a)–(c), respectively. Figures 4(g)–(i) show the line profiles along the ***E*** vector direction shown in Figs. 4(d)–(f), respectively. Figures 4(j) - (l) show the line profiles in the direction perpendicular to the ***E*** vector shown in Figs. 4(d)–(f), respectively. As shown in Fig. 4(g), after irradiation for 1000 pulses, periodic intervals spaced approximately 1.3 μm apart in the ***E*** vector direction are formed. As shown in Fig. 4(i), after 1500 pulses, the periodic intervals are approximately 1.0 μm in the ***E*** vector direction.

As shown in Figs. 4 (i) and (l), after 2000 pulses, nanoparticle periodic intervals of approximately 1.6 μm in the ***E*** vector direction and approximately 560 nm in the direction perpendicular to the ***E*** vector, respectively, were obtained. The periodic intervals perpendicular to the ***E*** vector direction are approximately equivalent to the wavelength of the laser beam.

Figure 5 shows the relationship between the average nanoparticle diameter and the number of laser pulses, where the error bar indicates the maximum and minimum nanoparticle diameter for each number of pulses. It can be seen that the average size of nanoparticles after irradiation of 1500 pulses was larger than that after 1000 pulses, but with increase in the number of pulses to 2000, the average nanoparticle size was observed to be smaller than that observed for 1000 pulses. As can be seen in Fig. 3 and Fig. 5, the absorption peak red-shifted with increasing the particle size, which is in agreement with the previous study [33].

As can be seen in Fig. 1, the surface of the deposited Au film is uneven. Because of uneven surface scattering, incident light turns into surface waves [24-25, 27]. Periodic modulation of the energy density incident on the Au film is the result of interference between the incident and surface waves. In regions of constructive interference, the Au film absorbs sufficient energy for nanoparticles to form. In regions of destructive interference, the Au film does not absorb sufficient energy for nanoparticles to form. In those interference enhanced regions, the Au film melts because the temperature increases rapidly during each short laser pulse, and so-called laser-induced dewetting takes place [21]. After the end of each laser pulse, the Au film rapidly cools down to room temperature and the Au film solidifies [21, 34]. By repeating the processes of

melting and resolidification induced by short laser pulses, periodic nanostructures are gradually formed with the continuous formation of Au nanoparticles in the interference enhanced regions. Finally, the periodic structures formed on the surface of the SiO_2 glass substrate resulting from the interference.

It has been reported that the direction of laser-induced periodic surface nanostructure formation is either parallel [24-25] or perpendicular [27-28] to the incident ***E*** vector. So far, we cannot give a comprehensive explanation of how the incident ***E*** vector direction influences the direction of periodic surface nanostructure formation. Clarification of this mechanism will be an interesting aspect of future work.

3.2 Examination of cross-sections after nanosecond-pulsed laser irradiation

To investigate the structures of the nanoparticles in detail, several cross-sectional TEM observations of sample 2 after laser irradiation of 1500 pulses were performed. The TEM specimens were prepared using FIB. Figure 6 shows a cross-sectional TEM image and EDS point analyses along the ***E*** vector direction. Figure 6(a) indicates that nanoparticles were obtained after laser irradiation. Figs. 6(b)–(d) show EDS point analysis of points ① through ③, which indicate the presence of Au nanoparticles on the SiO_2 glass substrate. We deposited the carbon layer as indicated C in Figure 6(a) on

the glass substrate as indicated SiO_2 in Figure (a) before the cross-sectional TEM specimen preparation by FIB to protect the surface of the nanostructure by Ga ion irradiation. However Ga atoms would be implanted in the specimen and remained the surface a little during the FIB processing. Therefore there is a strong Ga EDS peak in Figure 6(d).

Au nanoparticles not only formed on the surface of the SiO_2 glass substrate, but Au nanoparticles were also found to be embedded in the SiO_2 glass substrate. Figure 7(a) shows a cross-sectional TEM image of Au nanoparticles. Figures 7(b)–(e) show 2D EDS elemental mappings of the element concentrations observed in Fig. 7(a), which indicate the presence of Au nanoparticles partially embedded in the SiO_2 glass substrate.

Figure 8(a) shows a cross-sectional TEM image of a Au nanoparticle. According to Figures 8(b)–(e), which show the EDS elemental mapping measurement results, the Si elemental concentration is much less in the region of the Au nanoparticle than in the region surrounding the Au nanoparticle, which indicates that the Au nanoparticle is almost fully embedded in the SiO_2 glass substrate. Figure 8(f) shows the selected area diffraction pattern of the largest nanoparticle shown in Fig. 8(a). The selected area diffraction pattern confirms the nanoparticle to be a single crystal. Analysis of the diffraction pattern indicated that the single crystal was a face centered cubic structure.

Table 1 shows the calculation results of the lattice spacing and lattice constants derived from the diffraction pattern. The lattice constant was found to have an average value of $\bar{a}$=0.8520 nm.

As can be seen in the cross-sectional TEM images, Au nanoparticles over 160 nm in diameter were formed in the sample 2 after 1500 pulses irradiation. This is bigger than that of the Au nanoparticles in sample 1. It has been reported that as increasing the initial film thickness on the substrate, the diameter of nanoparticles may increase by short-pulsed laser irradiation [21]. The diameter of nanoparticles by short-pulsed laser irradiation would depend on not only laser irradiation conditions but also the initial film thickness.

The Au nanoparticles embedment in the glass substrate by high-temperature annealing has been reported and its mechanism has been studied in detail by Tanya Karakouz et al [35]. The mechanism of Au nanoparticle heat transfer to the glass substrate by nanosecond-pulsed laser irradiation has been also studied in detail by S. Hashimoto et al [30]. The glass substrate can be heating by thermal diffusion from the Au nanoparticles heated by nanosecond-pulsed laser irradiation [30]. Thus the Au nanoparticles would be embedded into the glass substrate by nanosecond-pulsed laser irradiation if the laser energy is sufficiently high. In addition, the SiO_2 glass substrate

cannot rise up to high-temperature by direct interaction of nanosecond-pulsed laser irradiation, because we used high purity SiO_2 glass substrates with 90% transmittance of 532 nm visible light in this study.

Conclusion

In this study, we have investigated the fabrication of Au nanoparticles by nanosecond-pulsed laser irradiation of Au films deposited on SiO_2 glass substrates.

Au periodic nanostructures on the surface of the SiO_2 glass substrate were formed after laser irradiation up to 2000 pulses; these nanostructures had periodicity both along and perpendicular to the ***E*** vector direction. The structures of Au nanoparticles were investigated in detail, and not only nanoparticle distributions on the surface of the SiO_2 glass substrate but also Au nanoparticles embedded in the SiO_2 glass substrate were observed.

A LSPR response for the Au nanoparticles/SiO_2 system was observed in photoabsorbance spectra, and the wavelength of the LSPR peak was determined by the average size of the Au nanoparticles.

References

[1] E. Hutter, J.H. Fendler, Exploitation of localized surface plasmon resonance, Adv.Mater. 16 (October (19)) (2004) 1685–1706.

[2] N. Nath, A. Chilkoti, A colorimetric gold nanoparticle sensor to interrogatebiomolecular interactions in real time on a surface, Anal. Chem. 74 (2002)504–509.

[3] L. Olofsson, T. Rindzevicius, I. Pfeiffer, M. Kall, F. Hook, Surface-based gold-nanoparticle sensor for specific and quantitative DNA hybridization detection,Langmuir 19 (2003) 10414–10419.

[4] A.J. Haes, R.P. Van Duyne, A unified view of propagating and localized surfaceplasmon resonance biosensors, Anal. Bioanal. Chem. 379 (2004) 920–930.

[5] T.-J. Lin, K.-T. Huang, C.-Y. Liu, Determination of organophosphorous pesticidesby a novel biosensor based on localized surface plasmon resonance, Biosens.Bioelectron. 22 (2006) 513–518.

[6] T.-J. Lin, M.-F. Chung, Detection of cadmium by a fiber-optic biosensor basedon localized surface plasmon resonance, Biosens. Bioelectron. 24 (2009)1213–1218.

[7] A. Prabhakar, S. Mukherji, A novel C-shaped, gold nanoparticle coated, embed-ded polymer waveguide for localized surface plasmon resonance baseddetection,

Lab Chip 10 (2010) 3422–3425.

[8] M.P. Singh, G.F. Strouse, Involvement of the LSPR spectral overlap for energytransfer between a dye and Au nanoparticle, J. Am. Chem. Soc. 132 (2010)9383–9391.

[9] K.-Y. Jung, F.L. Teixeira, R.M. Reano, Au/SiO_2 nanoring plasmon waveguides atoptical communication band, J. Lightwave Technol. 25 (September (9)) (2007).

[10] S. Sato, T. Arai, T. Morikawa, K. Uemura, T.M. Suzuki, H. Tanaka, T. Kajino,Selective CO_2 conversion to formate conjugated with H_2O oxidation utilizingsemiconductor/complex hybrid photocatalysts, J. Am. Chem. Soc. 133 (2011)15240–15243.

[11] X. Hu, D.G. Cahill, R.S. Averback, Nanoscale pattern formation in Pt thin filmsdue to ion-beam-induced dewetting, Appl. Phys. Lett. 76 (2000) 3215–3217.

[12] X. Hu, D.G. Cahill, R.S. Averback, Dewetting and nanopattern formation of thinPt films on SiO_2 induced by ion beam irradiation, J. Appl. Phys. 89 (2001)7777–7783.

[13] X. Hu, D.G. Cahill, R.S. Averback, In situ transmission electron microscopy studyof irradiation induced dewetting of ultrathin Pt films, J. Appl. Phys 93 (2003)165–169.

[14] S. Dhara, Sharat Chandra, P. Magudapathy, S. Kalavathi, B.K. Panigrahi, K.G.M.Nair, V.S. Sastry, C.W. Hsu, C.T. Wu, K.H. Chen, L.C. Chen, Blue luminescenceof Au nanoclusters embedded in silica matrix, J. Chem. Phys. 121 (2004)12595–12599.

[15] F. Ruffino, R. De Bastiani, M.G. Grimaldi, C. Bongiorno, F. Giannazzo, F. Roc-caforte, C. Spinella, V. Raineri, Self-organization of Au nanoclusters on the SiO_2 surface induced by 200 keV-Ar^+ irradiation, Nucl. Instrum. Meth. Phys. Res. B257 (2007) 810–814.

[16] A.L. Stepanov, Synthesis of silver nanoparticles in dielectric matrix by ionimplantation: a review, Rev. Adv. Mater. Sci. 26 (2010) 1–29.

[17] X. Meng, T. Shibayama, R. Yu, S. Takayanagi, S. Watanabe, Microstructure anal-ysis of ion beam-induced surface nanostructuring of thin Au film deposited on SiO_2 glass, J. Mater. Sci. 48 (2012) 920–928.

[18] X. Meng, T. Shibayama, R. Yu, S. Takayanagi, S. Watanabe, Shift of localizedsurface plasmon resonance by Ar-ion irradiation of Ag–Au bimetallic filmsdeposited on Al_2O_3 single crystals, Nucl. Instrum. Meth. Phys. Res. B (2013),http://dx.doi.org/10.1016/j.nimb.2013.05.036.

[19] X. Meng, T. Shibayama, R. Yu, S. Takayanagi, S. Watanabe, Ion irradiation

syn-thesis of Ag–Au bimetallic nanospheroids in SiO_2 glass substrate with tunablesurface plasmon resonance frequency, J. Appl. Phys. 114 (2013) 054308.

[20] N.B. Dahotre, S.P. Harimkar, Laser Fabrication and Machining of Materials,Springer Science, New York, 2008, pp. 34–66.

[21] S.J. Henley, J.D. Carey, S.R.P. Silva, Pulsed-laser-induced nanoscale island for-mation in thin metal-on-oxide films, Phys. Rev. B 72 (2005) 195408.

[22] C. Favazza, R. Kalyanaraman, R. Sureshkumar, Robust nanopatterning by laser-induced dewetting of metal nanofilms, Nanotechnology 17 (2006) 4229–4234.

[23] F. Ruffino, A. Pugliara, E. Carria, C. Bongiorno, C. Spinella, M.G. Grimaldi, Forma-tion of nanoparticles from laser irradiation Au thin film on SiO_2/Si: elucidationthe Rayleigh-instability role, Mater. Lett. 84 (2012) 27–30.

[24] A.E. Siegman, P.M. Fauchet, Stimulated wood's anomalies on laser-illuminatedsurfaces, IEEE J. Quantum Electron. 22 (1986) 1384–1403.

[25] A. Kiesow, S. Strohkark, K. Loschner, A. Heilmann, Generation of wavelength-dependent, periodic line pattern in metal nanoparticle-containing polymerfilms by femtosecond laser irradiation, Appl. Phys. Lett. 86 (2005)153111.

[26] C. Favazza, J. Krishna, H. Krishna, R. Kalyanaraman, R. Sureshkumar, Laser-induced short and long-range ordering of Co nanoparticles on SiO_2, Appl.

Phys.Lett. 88 (2006) 1531181.

[27] S. Watanabe, Y. Yoshida, S. Kayashima, S. Yatsu, M. Kawai, T. Kato, In situ obser-vation of self-organizing nanodot formation under nanosecond-pulsed laserirradiation on Si surface, J. Appl. Phys. 108 (2010) 103510.

[28] Y. Yoshida, S. Watanabe, Y. Nishijima, K. Ueno, H. Misawa, T. Kato, Fabrica-tion of Au/Si nanocomposite structure by nanosecond pulsed laser irradiation,Nanotechnology 22 (2011) 375607.

[29] S.H. Ko, Y. Choi, D.J. Hwang, C.P. Grigoropoulos, J. Chung, D. Poulikakos,Nanosecond laser ablation of gold nanoparticle films, Appl. Phys. Lett. 89 (2006)141126.

[30] S. Hashimoto, T. Uwada, M. Hagiri, R. Shiraishi, Mechanistic aspect ofsurface modification on glass substrates assisted by single shot pulsed laser-induced fragmentation of gold nanoparticles, J. Phys. Chem. C 115 (2011)4986–4993.

[31] Y. Golan, L. Margulis, I. Rubinstein, Vacuum-deposited gold films. I. Factorsaffecting the film morphology, Surf. Sci. 264 (1992) 312–326.

[32] F. Ruffino, M.G. Grimaldi, Atomic force microscopy study of the growth mech-anisms of nanostructured sputtered Au film on Si(1 1 1): evolution with filmthickness and annealing time, J. Appl. Phys. 107 (2010) 104321.

[33] S. Link, M.A. El-Sayed, Size and temperature dependence of the plasmon absorp-tion of colloidal gold nanoparticles, J. Phys. Chem. B 103 (1999) 4212–4217.

[34] M. Kaempfe, T. Rainer, K.-J. Berg, G. Seifert, H. Graener, Ultrashort laser pulseinduced deformation of silver nanoparticles in glass, Appl. Phys. Lett. 74 (1999)1200–1202.

[35] T. Karakouz, B.M. Maoz, G. Lando, A. Vaskevich, I. Rubinstein, Stabilizationof gold nanoparticle films on glass by thermal embedding, ACS Appl. Mater.Interfaces 3 (2011) 978–987.

Table 1. Lattice spacings as derived from the electron diffraction pattern given in Fig 8(b); the calculated lattice constants are also given in the third column. *d* represents the lattice spacings, and *a* represents lattice constant.

hkl	d/nm	a/nm
$1\bar{1}1$	0.4915	0.8513
$\bar{2}\bar{2}0$	0.3044	0.8609
$\bar{1}\bar{3}1$	0.2543	0.8434
$2\bar{2}2$	0.2461	0.8525

Figure captions

Fig. 1 SEM images of (a) sample 1, composed of a 20 nm Au film deposited on a 0.1 mm thick SiO_2 glass substrate; (b) sample 2, composed of a 30 nm Au film deposited on a 0.8 mm thick SiO_2 glass substrate prior to laser irradiation and (c) cross-sectional TEM image of 30 nm Au film deposited on SiO_2 glass substrate from sample 2.

Fig. 2 Optical microscope images of the Au(20 nm)/SiO_2(0.1 mm) system (sample 1) after laser irradiation with an energy density of 0.7 kJ/m^2 and a repetition rate of 2 Hz for (a) 1000, (b) 1500, and (c) 2000 pulses; (d) the Au(30 nm)/SiO_2(0.8 mm) system (sample 2) after laser irradiation with an energy density of 0.7 kJ/m^2 and a repetition rate of 2 Hz for 1500 pulses. ***E*** vector indicates the electric field vector of the laser light on the surface under laser irradiation.

Fig. 3 Photoabsorbance spectra of sample 1 after laser irradiation for (a) 1000, (b) 1500, and (c) 2000 pulses, and sample 2 after laser irradiation for (d) 1500 pulses.

Fig. 4 Upper column: SEM images of the Au(20nm)/SiO_2(0.1mm) system (sample 1) after laser irradiation with energy density of 0.7 kJ/m^2 and repetition rate of 2Hz for (a)1000, (b)1500,and (c)2000 pulses. Middle column: (d)-(f) The 2-dimensional Autocorrelation function (ACF) images obtained from squared part in (a)-(c), respectively. Lower column: (g)-(i) Line profiles along E vector direction in (d)-(f), respectively. (j)-(l) Line profiles along vertical to E vector direction in (d)-(f), respectively. E vector indicates the electric field vector of the laser light on the surface under laser irradiation.

Fig. 5 Average nanoparticle diameter versus number of laser pulses. The error bars indicate the maximum and minimum particle diameters.

Fig. 6 TEM image and EDS spectra of the laser irradiated Au(30nm)/SiO_2(0.8mm) system (sample 2) for 1500 pulses: (a) a bright field cross-sectional TEM image showing the three sample points examined by EDS, (b) EDS spectra at point ①, (c) EDS spectra at point ②, and (d) EDS spectra at point ③.

Fig. 7 TEM image and EDS mapping of the laser irradiated Au(30nm)/SiO_2(0.8mm) system (sample 2) for 1500 pulses: (a) bright-field cross-sectional TEM image showing Au nanoparticles half

embedded in the SiO_2 glass substrate, (b) EDS mapping of the Au distribution, (c) EDS mapping of the O distribution, (d) EDS mapping of the Si distribution, and (e) EDS mapping of the C distribution.

Fig. 8 TEM analysis results of the laser-irradiated Au(30nm)/SiO_2(0.8mm) system (sample 2) for 1500 pulses: (a) a bright-field cross-sectional TEM image showing an Au nanoparticle fully embedded in the SiO_2 glass substrate, (b) EDS mapping of the Au distribution, (c) EDS mapping of the O distribution, (d) EDS mapping of the Si distribution, and (e) EDS mapping of the C distribution, (g) the selected area electron diffraction pattern of the Au nanoparticle, the camera length is 600 mm.

Fig. 1

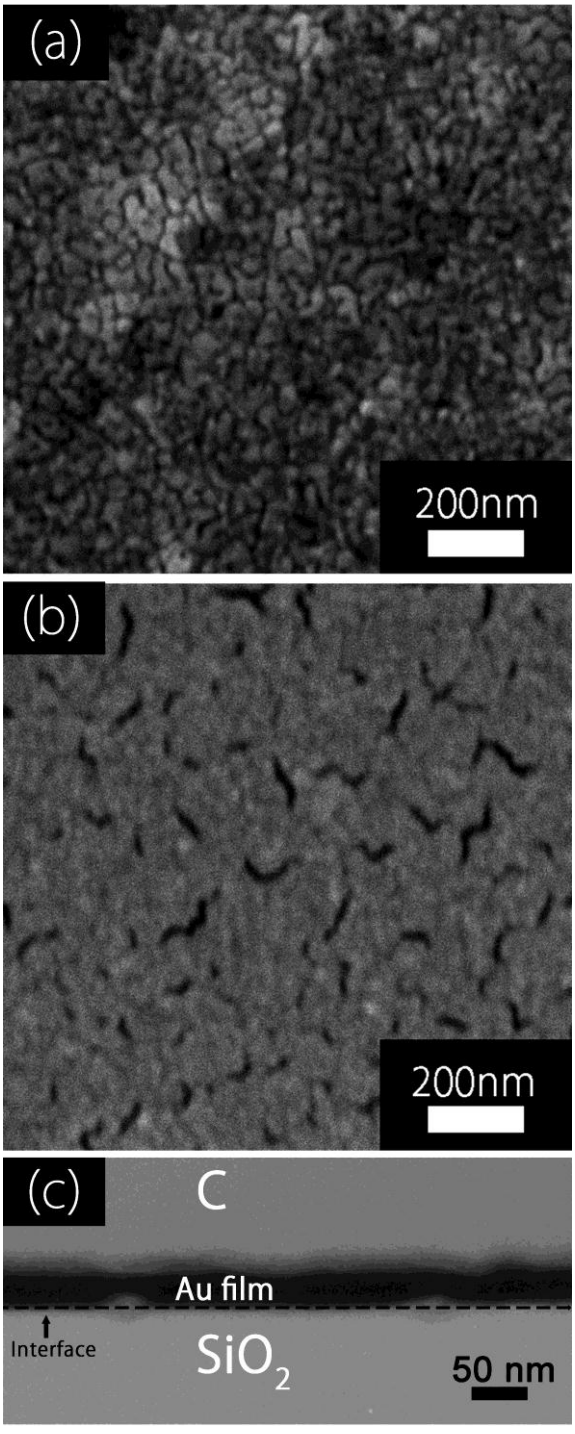

Fig. 2

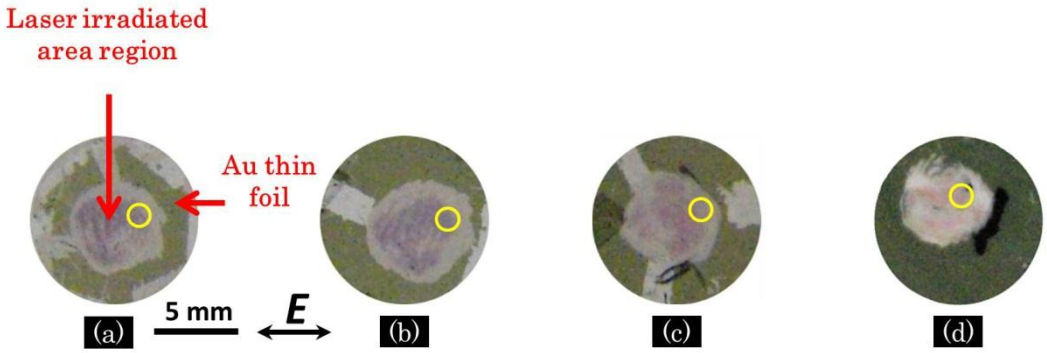

Fig. 3

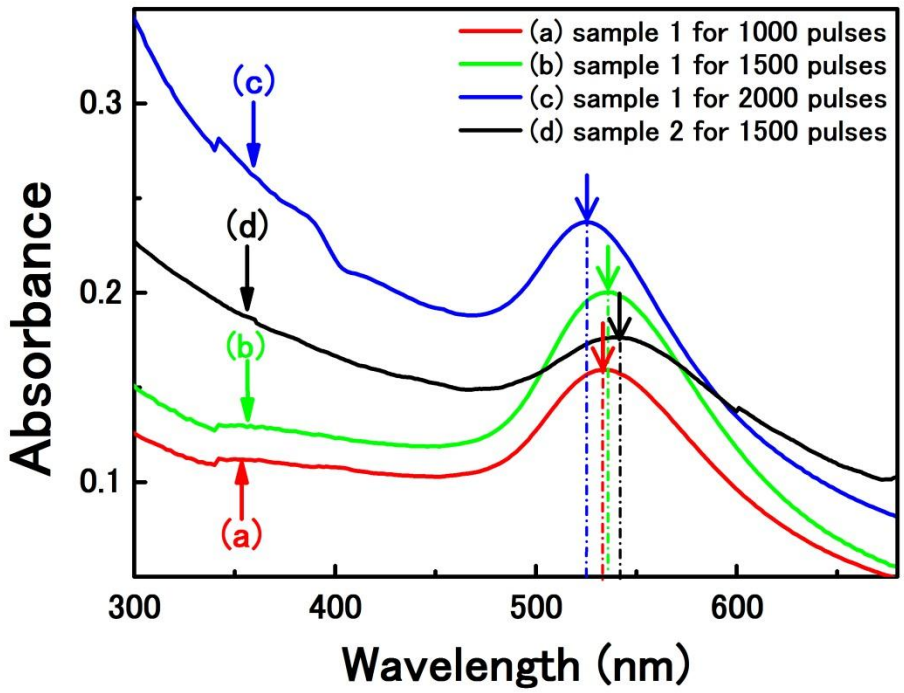
(a) sample 1 for 1000 pulses
(b) sample 1 for 1500 pulses
(c) sample 1 for 2000 pulses
(d) sample 2 for 1500 pulses
(c)
(d)
(b)
(a)
Absorbance
0.3
0.2
0.1
300
400
500
600
Wavelength (nm)

Fig. 4

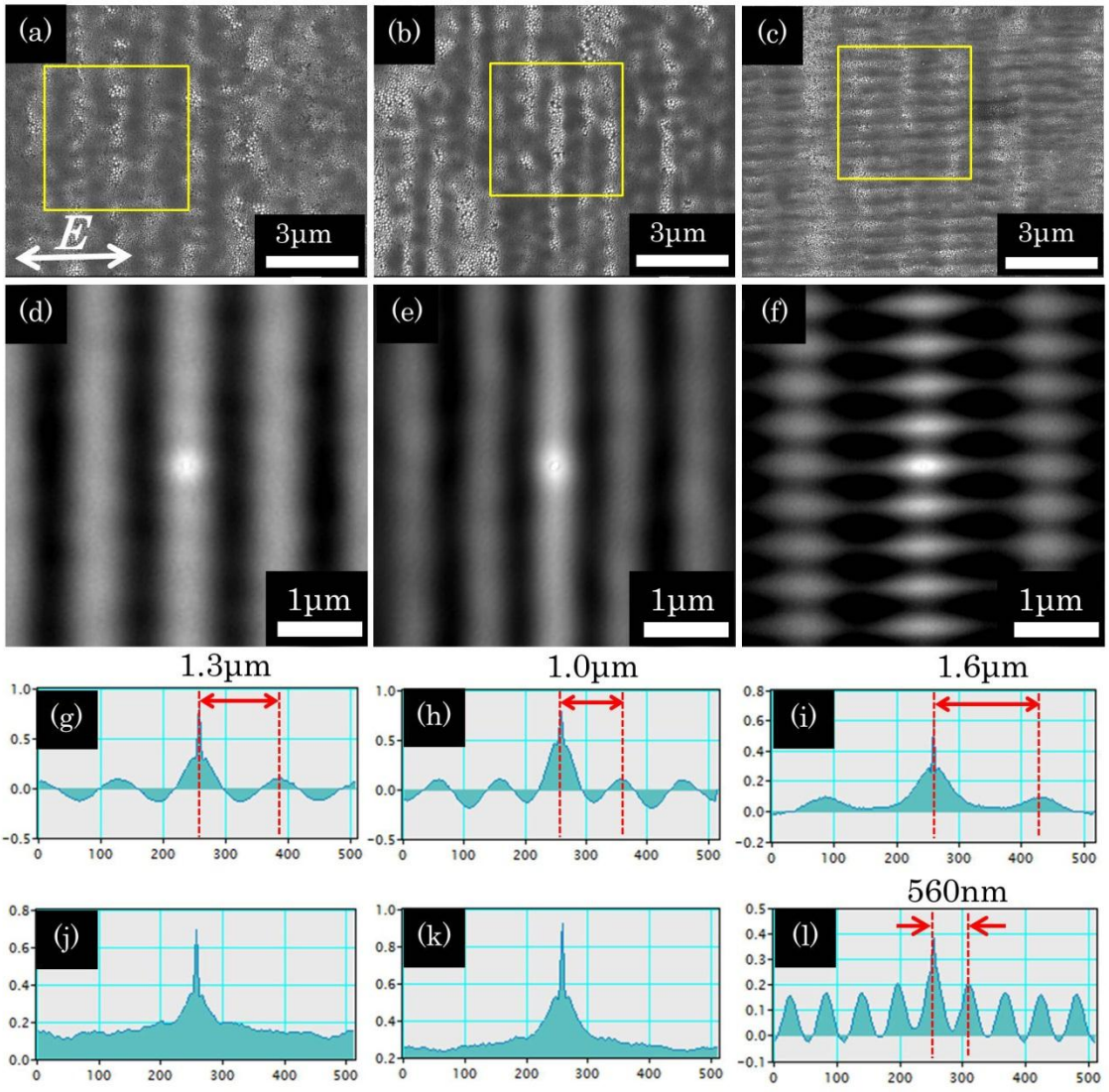

Fig. 5

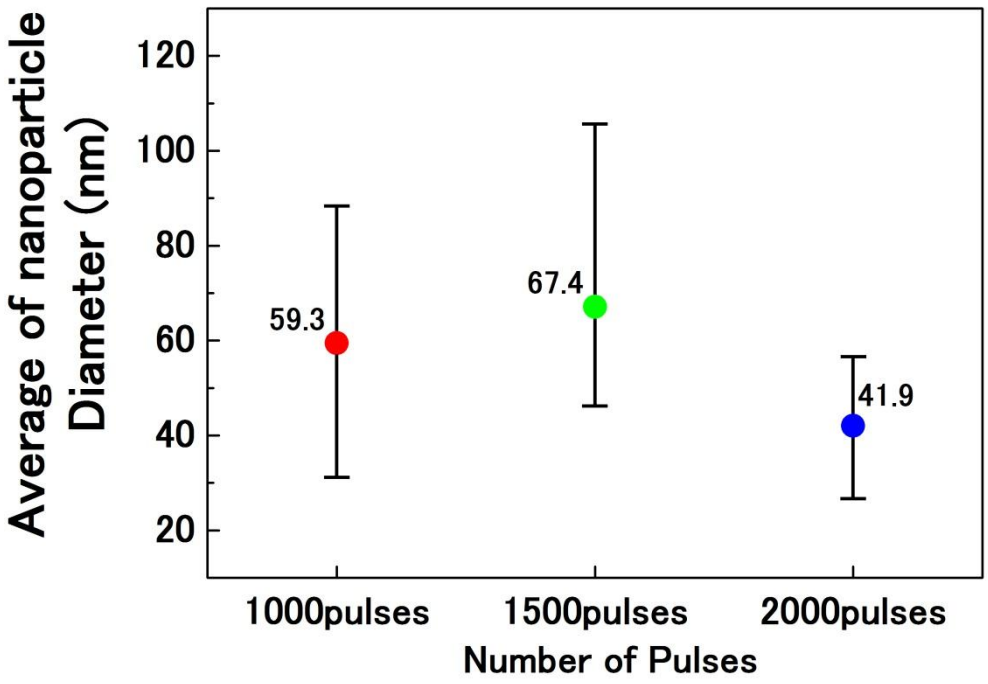
Average of nanoparticle Diameter (nm)
120
100
80
60
40
20
59.3
67.4
41.9
1000pulses
1500pulses
2000pulses
Number of Pulses

Fig. 6

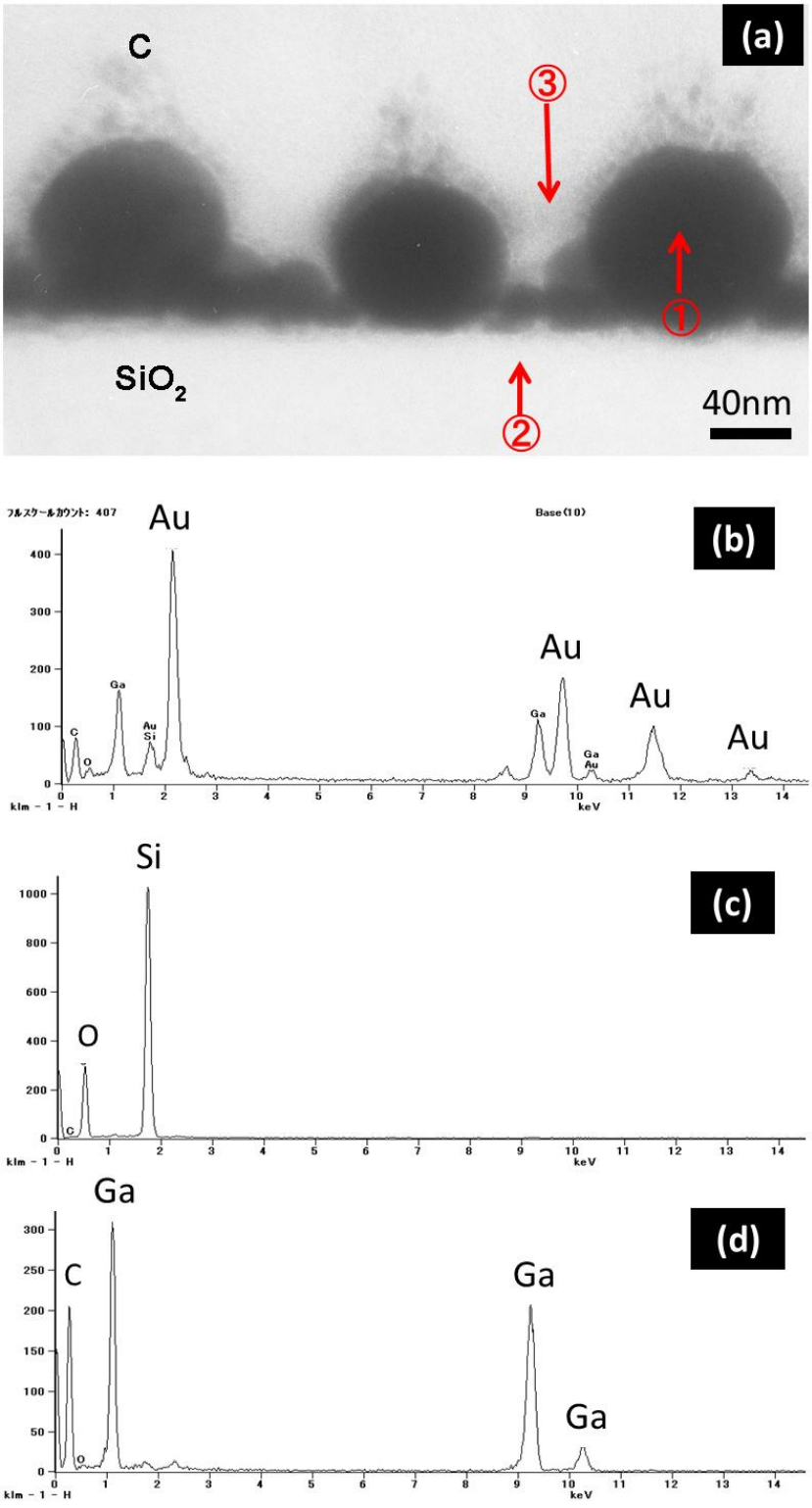
(a)
C
③
①
②
SiO2
40nm
(b)
Au
Au
Au
Au
Ga
Ga
C
O
Au
Si
Ga
Au
keV
(c)
Si
O
C
keV
(d)
Ga
C
Ga
Ga
O
keV

Fig. 7

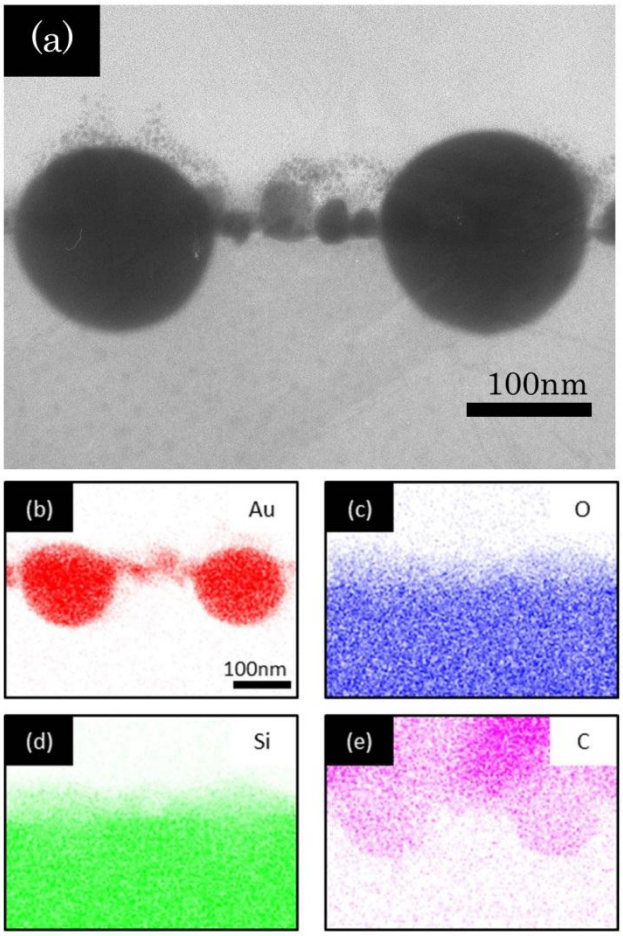

Fig. 8

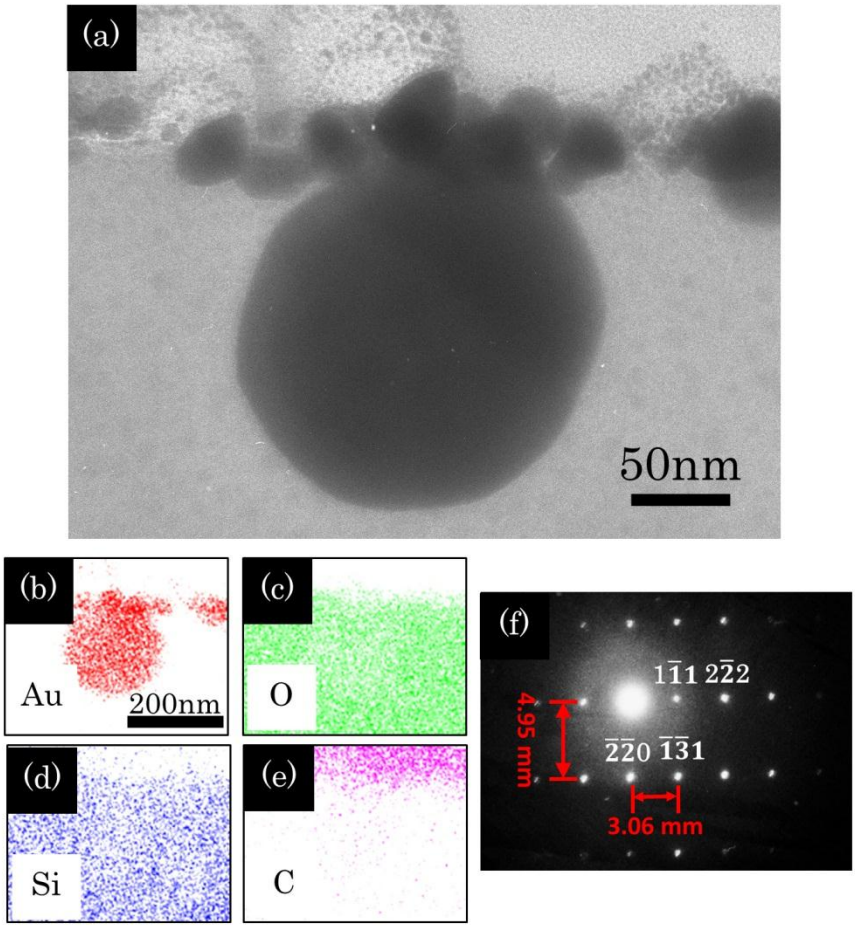
(a)
50nm
(b)
Au
200nm
(c)
O
(d)
Si
(e)
C
(f)
$1\bar{1}1$ $2\bar{2}2$
4.95 mm
$\bar{2}\bar{2}0$ $\bar{1}\bar{3}1$
3.06 mm